DOI: 10.1534/genetics.104.028035

The Amino Terminus of the *Saccharomyces cerevisiae* DNA Helicase Rrm3p Modulates Protein Function Altering Replication and Checkpoint Activity

Jessica B. Bessler and Virginia A. Zakian[1]

Department of Molecular Biology, Princeton University, Princeton, New Jersey 08544-1014

Manuscript received February 24, 2004
Accepted for publication July 28, 2004

ABSTRACT

The Pif1 family of DNA helicases is conserved from yeast to humans. Although the helicase domains of family members are well conserved, the amino termini of these proteins are not. The *Saccharomyces cerevisiae* genome encodes two Pif1 family members, Rrm3p and Pif1p, that have very different functions. To determine if the amino terminus of Rrm3p contributes to its role in promoting fork progression at >1000 discrete chromosomal sites, we constructed a deletion series that lacked portions of the 249-amino-acid amino terminus. The phenotypes of cells expressing alleles that lacked all or most of the amino terminus were indistinguishable from those of *rrm3*Δ cells. Rrm3p deletion derivatives that lacked smaller portions of the amino terminus were also defective, but the extent of replication pausing at tRNA genes, telomeres, and ribosomal DNA (rDNA) was not as great as in *rrm3*Δ cells. Deleting only 62 amino acids from the middle of the amino terminus affected only rDNA replication, suggesting that the amino terminus can confer locus-specific effects. Cells expressing a fusion protein consisting of the Rrm3p amino terminus and the Pif1p helicase domain displayed defects similar to *rrm3*Δ cells. These data demonstrate that the amino terminus of Rrm3p is essential for Rrm3p function. However, the helicase domain of Rrm3p also contributes to its functional specificity.

HELICASES harness the energy of nucleotide hydrolysis to separate the two strands of duplex nucleic acids. DNA helicases are essential for replication, recombination, and repair while RNA helicases play critical roles in transcription, RNA processing, and translation. Most DNA and RNA helicases contain seven motifs that are spread throughout a 200- to 700-amino-acid region (Gorbalenya and Koonin 1993). Because the seven helicase motifs are short and degenerate, their presence alone does not confer significant similarity upon two proteins that contain them. Rather, helicases are placed into families on the basis of more extensive sequence similarities that occur both within the helicase motifs and in other regions of the protein. For example, the *Saccharomyces cerevisiae* DNA helicase Rrm3p is a member of the Pif1 family of DNA helicases of which Pif1p is the prototype member. Pif1 family members have >30% similarity in all pairwise combinations over an ~400-amino-acid region that contains the helicase motifs (Zhou *et al.* 2000; Bessler *et al.* 2001). However, the amino termini of these homologs rapidly diverge (Figure 1; Zhou *et al.* 2000; Bessler *et al.* 2001), and the region carboxy terminal to the helicase domain varies in size and sequence.

[1]*Corresponding author:* Department of Molecular Biology, Lewis Thomas Labs, Princeton University, Princeton, NJ 08544-1014. E-mail: vzakian@molbio.princeton.edu

Although most eukaryotes encode only a single Pif1 family member, *S. cerevisiae* is one of several single-celled eukaryotes that encode two Pif1 family members. Pif1p and Rrm3p, as well as the single fission yeast Pif1 homolog, called Pfh1p, are 5′ to 3′ DNA helicases as determined by *in vitro* assays (Foury and Kolodynski 1983; Ivessa *et al.* 2000; Zhou *et al.* 2000; Zhou *et al.* 2002). At least for Rrm3p and Pfh1p, this *in vitro* helicase activity does not require the amino terminus of the protein.

Although the helicase domains of Pif1 homologs are highly similar, the members of this family do not have identical functions. The fission yeast Pfh1p is essential and appears to function in a late stage of chromosome replication (Tanaka *et al.* 2002; Zhou *et al.* 2002). In contrast, neither Pif1p nor Rrm3p is essential, and cells lacking both proteins are also viable (Schulz and Zakian 1994; Ivessa *et al.* 2000). Pif1p plays an important role in the maintenance of mitochondrial DNA (Foury and Kolodynski 1983) and also inhibits telomerase-mediated lengthening of telomeres (Zhou *et al.* 2000; Myung *et al.* 2001), while Rrm3p functions in semiconservative replication of chromosomal DNA. In the absence of Rrm3p, replication forks pause at an estimated 1400 discrete sites, including telomeres, tRNA genes, centromeres, inactive replication origins, transcriptional silencers, and multiple sites within the ribosomal DNA (rDNA; Ivessa *et al.* 2000, 2002, 2003). The helicase activity of Rrm3p is required for its role in fork progression (Ivessa *et al.* 2000, 2002). Rrm3p-dependent sites occur

TABLE 1

***S. cerevisiae* strains used in this study**

Strain	Genotype	Reference or source
VPS106	*MAT***a** *ade2 ade3 leu2-3 112 ura3*Δ *trp1*Δ *lys2-801 can1*	Schulz and Zakian (1994)
VPS106 *rrm3* UT	*rrm3*::*TRP1* VII-L.::*URA3*	Ivessa *et al.* (2000)
JBB44	VPS *rrm3*::*TRP1 fob1*::*URA3*-HA	Torres *et al.* (2004a)
YPH501	*MAT***a**/α *ura3-52 lys2-801 ade2-101 trp1*-Δ*63 his3*-Δ*200 leu2*-Δ*1*	Sikorski and Hieter (1989)
JZT121	YPH501 *RRM3/rrm3*::*HIS3 SRS2/srs2*::*TRP1*	Torres *et al.* (2004b)
JZT254	YPH501 *RRM3/rrm3*::*HIS3 RAD50/rad50*::*TRP1*	Torres *et al.* (2004b)
JZT630	YPH501 *RRM3/rrm3*::*HIS3 MEC1/mec1*::HA *SML1/sml1*::*TRP1*	Torres *et al.* (2004b)
JZT531	VPS106 *rrm3*::*hygromycin* Fob1p-13Myc	J. Z. Torres

where stable, nonnucleosomal protein complexes are bound to DNA. Disruption of these complexes eliminates dependence upon Rrm3p, leading to the proposal that Rrm3p promotes fork movement past nonnucleosomal protein-DNA complexes (Ivessa *et al.* 2003; Torres *et al.* 2004a).

The role of Rrm3p in fork progression has also been found to contribute to genome integrity, as its absence is correlated with replication fork breakage (Ivessa *et al.* 2000, 2002, 2003), site-specific increases in recombination (Ivessa *et al.* 2000, 2002, 2003; Keil and McWilliams 1993), and elevated Ty transposition (Scholes *et al.* 2001). The stalled and broken forks that accumulate in *rrm3*Δ cells activate DNA checkpoints, as demonstrated by the hyperphosphorylation of Rad53p, an effector kinase for both the DNA damage and the intra-S-phase checkpoints (Ivessa *et al.* 2003; Torres *et al.* 2004b). Although *rrm3*Δ cells are viable, this viability requires the ability to activate DNA checkpoints. For example, *rrm3*Δ cells that also lack Mec1p, the sensor kinase for DNA checkpoints, are inviable at low temperatures (Ivessa *et al.* 2003). Likewise, when *RRM3* is deleted in conjunction with other genes encoding repair and checkpoint proteins, including *SRS2* and *RAD50*, the doubly mutant strains are not viable (Ivessa *et al.* 2003; Ooi *et al.* 2003; Weitao *et al.* 2003; Schmidt and Kolodner 2004; Torres *et al.* 2004b). This loss of viability is likely due to the inability to detect or repair the damage caused by *rrm3*Δ-dependent replication fork stalling.

Although the *S. cerevisiae* Pif1 and Rrm3 proteins are 40% identical and 60% similar over their helicase domains, their ~250-amino-acid amino termini have almost no similarity. The amino termini of helicases can serve a variety of functions. For example, the amino terminus of the human RecQ family Werner's helicase has an exonuclease domain (Huang *et al.* 1998; Suzuki *et al.* 1999), while the amino terminus of the *S. cerevisiae* RecQ homolog Sgs1p helicase interacts with topoisomerase III (Gangloff *et al.* 1994; Bennett *et al.* 2000) and may have an additional function that is independent of the helicase domain (Mullen *et al.* 2000). In other helicases, the amino terminus can recruit the helicase to its site of action or promote dimerization (Wang and Guthrie 1998; Schneider and Schwer 2001; Ziegelin *et al.* 2003). The amino termini of Pif1p, Rrm3p, and Pfh1p encode a signal sequence for mitochondrial import, although its functionality has been demonstrated only for Pif1p (Figure 1; M. K. Mateyak and V. A. Zakian, unpublished results; Schulz and Zakian 1994; Zhou *et al.* 2000, 2002). Additionally, the amino terminus of Rrm3p contains a putative PCNA interaction motif and interacts with PCNA by yeast two-hybrid and *in vitro* translation assays (Figure 1; Schmidt *et al.* 2002).

In this article, we examine the function of the 249-amino-acid amino-terminal region of Rrm3p. Although the amino terminus of Rrm3p is not required for helicase activity *in vitro* (Ivessa *et al.* 2002), this region was essential for the replication function of Rrm3p *in vivo* as well as for regulation of protein abundance. Additionally, deletion of internal portions of the amino terminus altered Rrm3p function, both diminishing its replication activity and causing new phenotypes. The helicase domain of Rrm3p likely also contributes to *in vivo* specificity, as a hybrid protein having the amino- and carboxy-terminal regions of Rrm3p fused to the helicase domain of Pif1p was unable to supply the replication activity of Rrm3p. Amino-terminal deletion alleles that had some but not all of the replication defects of *rrm3*Δ cells did not activate Rad53p nor did they require the *MEC1*, *SRS2*, or *RAD50* genes for viability. Together, these results support a model in which a threshold of stalled replication forks must be surpassed to activate the intra-S-phase checkpoint.

MATERIALS AND METHODS

Yeast strains and methods: Yeast strains used are *rrm3*Δ derivatives of VPS106 (Schulz and Zakian 1994; Ivessa *et al.* 2000) or YPH499 (Sikorski and Hieter 1989). In each experiment, these derivatives carried the centromere plasmid YCplac111 or the 2μ plasmid YEplac181. These plasmids were used to express Rrm3p and the deletion allele series. The full-length Rrm3p was expressed from an ~3300-bp fragment, which contains 467 bp of sequence upstream of the start of the open reading frame. All deletion alleles carried the same amount of upstream sequence. Western analysis and two-dimensional gel electrophoresis (2D gels) were done in VPS

TABLE 2

Plasmids used in this study

Name	Insert	Reference or source
YCplac111	CEN4 ARS1 *LEU2*	Gietz and Sugino (1988)
pJB5[a]	*RRM3*	J. B. Bessler; Ivessa *et al.* (2002)
pJB108[a]	*RRM3*gly8Myc9	This study
pJB61[a]	*rrm3*Δ3-139	This study
pJB104[a]	*rrm3*Δ3-139gly8Myc9	This study
pJB67[a]	*rrm3*Δ134-196	This study
pJB105[a]	*rrm3*Δ134-196gly8Myc9	This study
pJB72[a]	*rrm3*Δ121-211	This study
pJB106[a]	*rrm3*Δ121-211gly8Myc9	This study
pJB75[a]	*rrm3*Δ53-202	This study
pJB107[a]	*rrm3*Δ53-202gly8Myc9	This study
pJB134[a]	*rrm3*Δ2-249gly8Myc9	This study
pJB133[a]	*rrm3*Δ2-234gly8Myc9	This study
pJB135[a]	*rrm3*Δ2-218gly8Myc9	This study
pJB140[a]	*rrm3*Δ2-194gly8Myc9	This study
pJB141[a]	*rrm3*Δ2-177gly8Myc9	This study
pIA20	*RRM3 ADE3 URA3* CEN4 ARS1	Ivessa *et al.* (2003)
YEplac181	2μ *LEU2*	Gietz and Sugino (1988)
pJB121[b]	*RRM3*	This study
pJB118[b]	*rrm3*Δ134-196	This study

[a] Plasmid backbone is YCplac111.
[b] Plasmid backbone is YEplac111.

strains, except for the *Stu*I gels, which were done with YPH strains. Cell viability assays were done in the *rrm3*Δ YPH strains with deletions of other genes made as described (Torres *et al.* 2004a,b). Chromatin immunoprecipitation (ChIP) was done in VPS strains carrying Fob1-13Myc. Strains and plasmids used in this study are listed in Tables 1 and 2, respectively.

Construction of Rrm3p mutant alleles: A *Pst*I fragment containing *RRM3* was obtained from the L3000 plasmid, a gift from Ralph Keil (Keil and McWilliams 1993), and cloned into YCplac111 (Gietz and Sugino 1988). The *rrm3*Δ2-249, *rrm3*Δ2-234, *rrm3*Δ2-218, *rrm3*Δ2-194, and *rrm3*Δ2-177 alleles were made by using site-directed mutagenesis to convert the start codon of Rrm3p to an *Nde*I site (Mullen *et al.* 2000). Another *Nde*I site was created at the position of various methionines (amino acids 234, 218, 194, and 177). At amino acid 249, an *Nde*I site was engineered without a methionine codon present. The region between the two *Nde*I sites was removed by digestion with *Nde*I and the rest of the plasmid was gel purified and then religated. The junctions were sequenced to ensure that proper ligation had occurred. The other deletions were made by digesting L3000 with *Avr*II (*rrm3*Δ3-139) or *Spe*I (*rrm3*Δ134-196, *rrm3*Δ121-211, and *rrm3*Δ53-202) followed by BAL31 digestion with aliquots taken at different time points. BAL31-digested DNA was religated and sequenced to identify in frame deletions. Once deletion alleles were obtained they were cloned into YCplac111.

The Rrm3-Pif1 fusion protein was constructed by digesting YCplac111-*RRM3* or YEplac181-*RRM3* with *Age*I. The digested DNAs plus a PCR fragment containing the Pif1p helicase domain flanked by sequence from the Rrm3p amino terminus and the Rrm3p carboxyl terminus were cotransformed into an *rrm3*Δ derivative of VPS. Recombination in yeast between the *RRM3* sequences flanking the *PIF1* DNA in the PCR fragment and the *RRM3* sequences on the plasmid generated the fusion protein.

Myc epitope tags and chromatin immunoprecipitation: Myc tagging was carried out as described in Wellinger *et al.* (1996), except an eight-glycine linker was placed between the nine Myc epitopes and the carboxyl terminus of Rrm3p. Fob1p-13Myc was made by J. Torres as described in Longtine *et al.* (1998). Southern blots and Western blots were used to confirm correct tagging and protein expression. ChIPs were done as described in Wellinger *et al.* (1996) and Taggart *et al.* (2002) except that Protein G Dynabeads (Dynal) were used and sonication levels were increased. DNA immunoprecipitated from Myc-tagged Fob1p was amplified using 23 cycles of multiplex PCR with a primer set surrounding the replication fork barrier (RFB) (RFB+ CTCTGGAACTTGCCATCATCA TTC, RFB− GCAAAGATGGGTTGAAAGAGAAGG) and another set flanking an internal region of 35S (35S+ TTGACT TACGTCGCAGTCCTCAGT, 35S− AGGACGTCATAGAGGG TGAGAATC). Fold enrichment was quantitated using Eagle Eye images of gels, densitometric analysis with NIH Image 1.60, and the following equation: fold enrichment of Fob1p = (Myc tag RFB/no tag RFB) × (no tag 35S/Myc tag 35S).

Cell viability assays: Heterozygous *RRM3*/*rrm3*Δ strains were constructed and the deletion was covered using pIA20, a *URA3* plasmid containing wild-type *RRM3*. The second gene of interest was then deleted. Strains were sporulated and spores with the desired genotype and carrying the plasmid were recovered (Torres *et al.* 2004b). *rrm3* alleles were transformed into these haploid strains on *LEU2* plasmids. Strains carrying both plasmids were streaked to complete media lacking leucine (YC-LEU) to allow for the loss of the *URA3* plasmids. After 2 days, cells were streaked onto YC-LEU 5-fluoroorotic acid (5-FOA) plates and grown for 3 days at 23° (*mec1*Δ *sml1*Δ *rrm3*Δ) or 2 days at 30° (all other strains).

Protein isolation, Western blotting, and gel methods: Protein isolation and Western blotting was done using a TCA method adopted from Pellicioli *et al.* (1999) as described in Ivessa *et al.* (2003). A wet electrophoretic transfer in phosphate buffer was used to transfer protein to nitrocellulose membranes, which were probed with anti-Rad53p (gift of J. Diffley), anti-Myc, or anti-actin (gift from M. Rose of antiserum

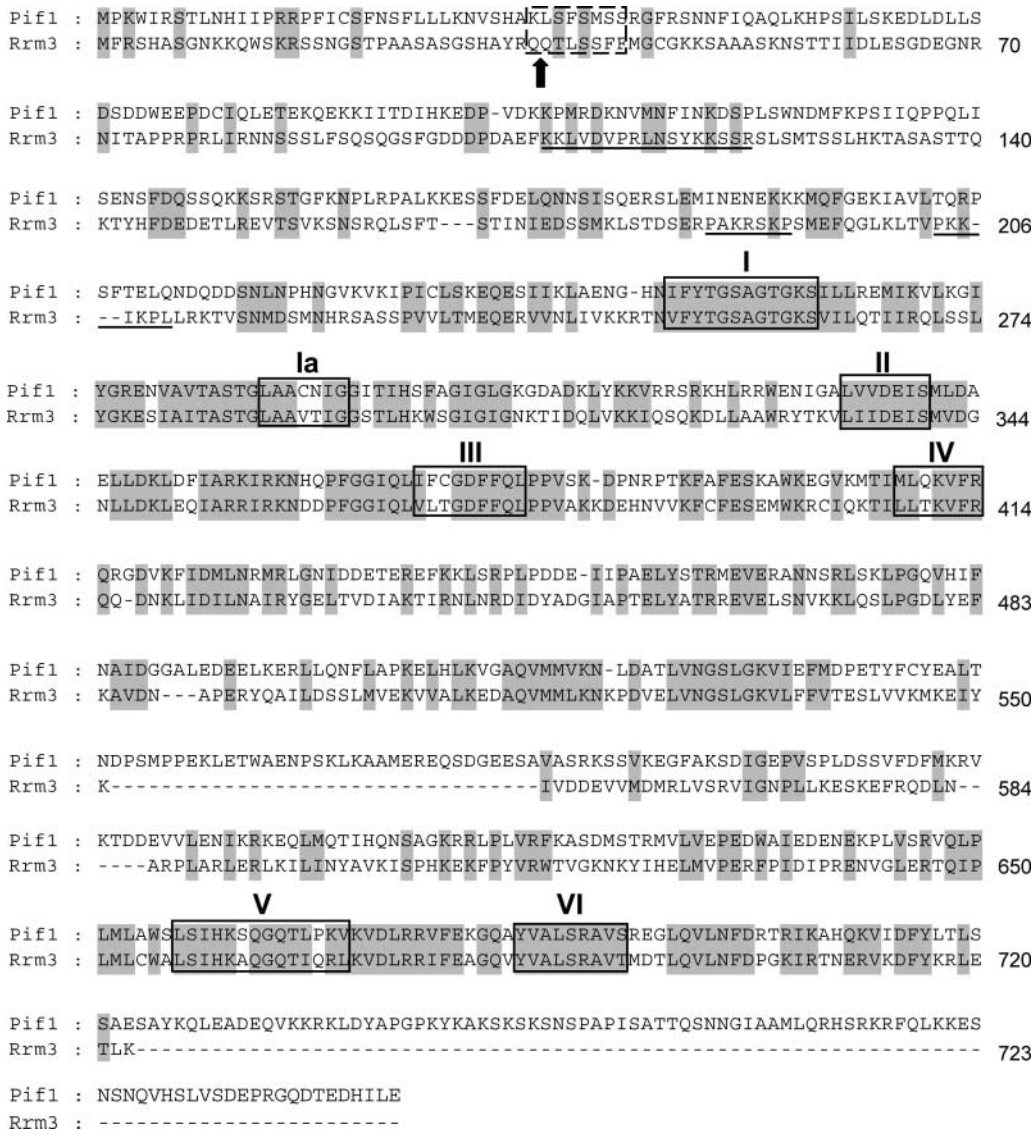

FIGURE 1.—Rrm3p is a member of the Pif1 family of DNA helicases; alignment of Rrm3p with Pif1p is shown. Dashes indicate gaps in the alignment. Conserved residues are in gray; numbers refer to Rrm3p amino acids. The positions of the seven helicase motifs are indicated with black boxes and roman numerals. The dashed box outlines the proposed site of PCNA interaction (WARBRICK 2000; SCHMIDT *et al.* 2002). *RRM3* is predicted to encode both nuclear and mitochondrial forms of the protein (M. K. MATEYAK and V. A. ZAKIAN, unpublished results); the arrow indicates the predicted cleavage site for removing the mitochondrial signal sequence. The putative NLSs are underlined.

made by T. Wang and A. Bretscher). All 2D gels were done as described by IVESSA *et al.* (2000, 2002, 2003).

Sequence alignments: Rrm3p and Pif1p sequences were obtained from the Saccharomyces Genome Database (www.yeastgenome.org). The protein alignment was done using ClustalW default parameters online at www.ebi.ac.uk/clustalw/#. The alignment was imported into GeneChoice software for presentation (www.psc.edu/biomed/genedoc; NICHOLAS and NICHOLAS 1997).

RESULTS

The Rrm3p amino terminus negatively regulates Rrm3p abundance: Rrm3p is 723 amino acids long and the first helicase motif starts at amino acid 250 (Figure 1). To determine the contribution of the amino terminus to the *in vivo* functions of Rrm3p, we constructed a series of deletions that removed different amounts of the amino terminus (Figure 2A). The deletion alleles were modified such that the proteins carried nine Myc epitopes at the carboxyl end. This addition does not impair the ability of full-length Rrm3p to promote replication fork progression by the criterion of 2D agarose gel electrophoresis (J. B. BESSLER, J. Z. TORRES and V. A. ZAKIAN, unpublished results). The *rrm3*Δ2-249 allele is a complete deletion of the amino terminus while *rrm3*Δ2-234, *rrm3*Δ2-218, *rrm3*Δ2-194, and *rrm3*Δ2-177 compose a series of smaller amino-terminal deletions (numbers refer to deleted amino acids; *i.e.*, *rrm3*Δ2-249 lacks amino acids 2–249) (Figures 1 and 2A). We also constructed four alleles with more internal deletions in the amino terminus (*rrm3*Δ3-139, *rrm3*Δ134-196, *rrm3*Δ121-211, and *rrm3*Δ53-202). In Figure 2B, the different amino-terminal deletion mutants are grouped into three classes based upon their overall phenotypes, as determined by the experiments reported in this article.

Before examining the phenotypes of cells expressing

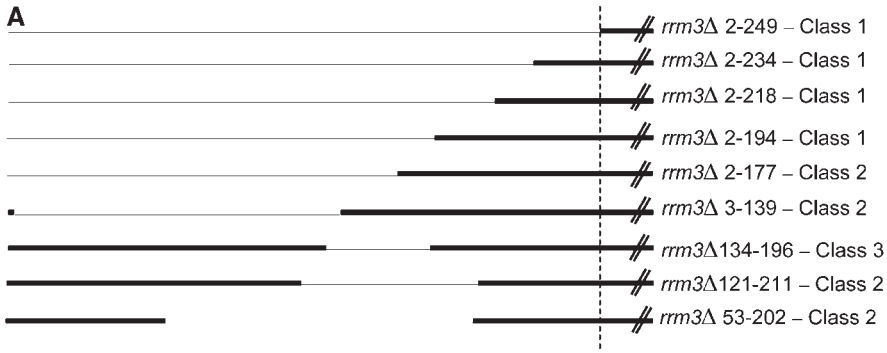

B ***rrm3* Allele Phenotypes**

Allele (Class)	Protein	Rad53p	*rad50Δ rrm3Δ srs2Δ rrm3Δ mec1Δ rrm3Δ*	tRNA	VII-L telomere	VII-L *adh4*	rDNA
RRM3	1	+	+	+	+	+	+
*rrm3*Δ	0	-	-	-	-	-	-
*rrm3*Δ2-249 (1)	10-100	-	-	-	-	-	-
*rrm3*Δ2-234 (1)	~100	-	-	-	-	-	-
*rrm3*Δ2-218 (1)	10-100	-	-	-	-	-	-
*rrm3*Δ2-194 (1)	10-100	-	-	-	-	-	-
*rrm3*Δ2-177 (2)	10-100	+	+	+/-	-	+	+/-
*rrm3*Δ3-139 (2)	10-100	+	+	+/-	-	+	+/-
*rrm3*Δ134-196 (3)	~10	+	+	+	+	+	RFB
*rrm3*Δ121-211 (2)	~10	+	+	+/-	-	+	+/-
*rrm3*Δ53-202 (2)	~10	+/-	+	+/-	-	+	+/-

FIGURE 2.—Structure and summary of phenotypes of *rrm3* deletion alleles. (A) Amino-terminal deletions of Rrm3p. Deletion alleles are named according to the amino acids removed. The amino terminus of Rrm3p is 249 amino acids long. Full-length Rrm3p is 723 amino acids. The dashed vertical line indicates the end of the amino terminus and the beginning of the helicase domain. Thick lines are the regions of the protein that are present and thin lines indicate the regions deleted. (B) The nine alleles are divided into three classes based upon the phenotypes described in this article, which are summarized here. Plus indicates a wild-type phenotype; minus indicates the null phenotype; +/− indicates an intermediate phenotype; RFB indicates a novel perturbation at the RFB. The protein column indicates a rough estimate of protein levels, with the wild-type level defined as one.

these amino-terminal deletion alleles, we first established that each mutant protein was expressed. All alleles, including wild-type *RRM3*, were cloned into the *LEU2* centromere plasmid YCplac111 and expressed as Myc-tagged proteins under the control of the *RRM3* promoter in an *rrm3*Δ strain. Proteins were prepared from equivalent numbers of log phase cells for each strain, separated by electrophoresis, and visualized by Western analysis using anti-Myc antibody (Figure 3; asterisks indicate expected positions for full-length proteins). For ease of comparison, we loaded 1:10 (Figure 3A), 1:30 (Figure 3B), and 1:100 (Figure 3C) dilutions of extract from strains expressing the deletion alleles. Membranes were stripped and reprobed with an anti-actin antibody to verify that extracts from the deletion strains contained similar amounts of protein. The extracts from the *RRM3* and the *rrm3*Δ strains were not diluted.

All of the deletion alleles produced stable protein (Figure 3). In fact, all of the terminally deleted mutant proteins were overexpressed relative to wild-type Rrm3p. In some cases, degradation products, in addition to full-length protein, were detected. Because these degradation products were not detected by antiserum to the amino terminus of Rrm3p, they are consistent with Rrm3p being degraded or cleaved within its amino terminus (data not shown). By comparing Westerns from 10-, 30-, and 100-fold serially diluted proteins (Figure 3), we estimate that *rrm3*Δ134-196, *rrm3*Δ121-211, and *rrm3*Δ53-202 were expressed at levels that were roughly 10-fold higher than the wild-type level, while *rrm3*Δ2-234 was expressed up to 100 times higher than the wild-type level. Alleles *rrm3*Δ2-249, *rrm3*Δ2-218, *rrm3*Δ2-194, *rrm3*Δ2-177, and *rrm3*Δ3-139 were >10-fold but <100-fold overexpressed (summarized in Figure 2B). Comparable or even much higher overexpression is seen for amino-terminally truncated versions of the *S. cerevisiae* Sgs1p DNA helicase (MULLEN *et al.* 2000). Although very high levels of overexpression of full-length Rrm3p from a GAL promoter cause slow growth (J. Z. TORRES and V. A. ZAKIAN, unpublished results), none of the strains expressing the amino-terminal *rrm3* deletion alleles had obvious growth defects (data not shown). Since all of the mutant alleles

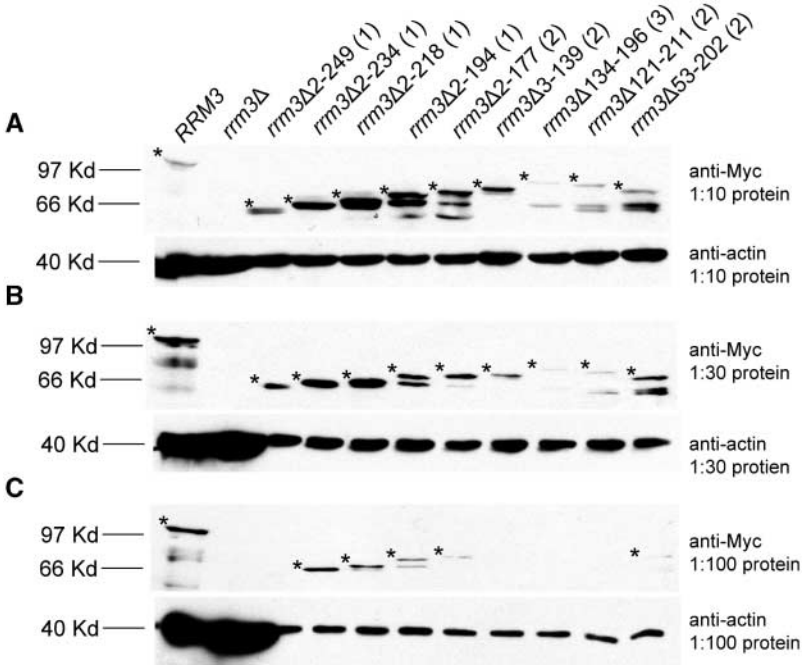

FIGURE 3.—The Rrm3p amino terminus negatively regulates protein abundance. For each strain, proteins were extracted from equal numbers of cells, diluted as indicated, separated by SDS-PAGE, and analyzed by Western blotting using a monoclonal anti-Myc antibody (BD Biosciences Clonetech). The same membranes were also probed with anti-actin antibody to establish that similar amounts of protein were loaded for each of the strains expressing *rrm3* deletion alleles. Positions of molecular weight markers are indicated. For each allele, the expected position of full-length protein is marked with an asterisk. In each strain, the YCplac111 plasmid alone or carrying an allele expressed from the *RRM3* promoter was introduced into an *rrm3*Δ strain. (A) A 1:10 dilution of protein extract was loaded for all lanes except the lanes with extracts from *RRM3* (lane 1) and *rrm3*Δ (lane 2) cells; *i.e.*, 10 times more *RRM3* and *rrm3*Δ extract was loaded compared to the amount from each of the deletion alleles. (B) 1:30 dilutions of mutant protein extracts. (C) 1:100 dilutions of mutant protein extracts. Protein abundance was estimated from these gels. Note the band visible for *rrm3*Δ2-218 is a doublet. Western exposure times were varied according to the dilution level of the extracts from the *rrm3* deletion alleles.

are expressed, any mutant phenotypes are not due to lack of protein. In addition, we conclude that the amino terminus negatively regulates protein levels.

Replication fork progression is altered in Rrm3p amino-terminal deletion alleles: In the absence of Rrm3p, replication forks slow or stall at ~1400 discrete sites, including tRNA genes, telomeres, and multiple sites within the rDNA array (IVESSA *et al.* 2000, 2002, 2003). These replication defects are detected using 2D agarose gel electrophoresis (BREWER and FANGMAN 1987). After separation by 2D gels, nonlinear replication intermediates migrate more slowly than linear molecules of the same mass. In an asynchronous culture, most DNA molecules are nonreplicating and form a large spot (1*N* spot) on the arc of linear molecules (Figure 4.1; arc of linears is indicated with a dashed line). Simple forked replication intermediates will emanate from the 1*N* spot and become increasingly nonlinear until the fork reaches the midpoint of the fragment (Figure 4.1; arc of replication intermediates is indicated with a solid line). As replication progresses, the forked intermediates become increasingly linear in shape until they reenter the arc of linear molecules when their replication is almost complete and their mass is close to 2*N*. When replication forks are slowed or stopped at a specific site, they generate an area of more intense hybridization on the arc of replication intermediates at the site of pausing (Figure 4.1; pause site indicated by an arrow).

To determine if the amino-terminal *rrm3* deletion alleles can supply the replication functions of Rrm3p, genomic DNA was isolated from asynchronous cultures, digested with the appropriate restriction enzyme, separated on 2D gels, and analyzed by Southern blotting. We examined replication of an alanine tRNA gene ($tRNA^A$, tA[AGC]F), the left telomere of chromosome VII, and the rDNA in each of the nine amino-terminal deletion mutants. On the basis of their patterns of replication through these three DNA substrates, the mutants fell into three classes. Four mutants had replication phenotypes indistinguishable from that of *rrm3*Δ cells (class 1); four mutants were defective in replication but not as defective as *rrm3*Δ cells (class 2); one mutant had wild-type or nearly wild-type replication at $tRNA^A$ and telomere VII-L but a novel replication pattern in the rDNA (class 3; summarized in Figure 2B). For ease of presentation, we show the results for only one mutant from each of the three classes for each DNA substrate.

Even in wild-type cells, replication forks pause at $tRNA^A$ (DESHPANDE and NEWLON 1996; Figure 4.2; indicated by arrow), but this pausing is increased dramatically in *rrm3*Δ cells (IVESSA *et al.* 2003; Figure 4.3). In addition, structures with the mobility expected for breakage of these stalled forks were detected (MARTIN-PARRAS *et al.* 1992; Figure 4.3; indicated with asterisk). The pattern of $tRNA^A$ replication in cells carrying class 1 alleles (*rrm3*Δ2-249, *rrm3*Δ2-234, *rrm3*Δ2-218, and *rrm3*Δ 2-194) was indistinguishable from that seen in *rrm3*Δ cells (Figure 4.4). In the four class 2 mutants (*rrm3*Δ2-177, *rrm3*Δ3-139, *rrm3*Δ121-211, and *rrm3*Δ53-202), the extent of pausing at $tRNA^A$ was intermediate between that seen in wild-type and *rrm3*Δ cells (Figure 4.5). In addition, replication fork breakage was not detected in

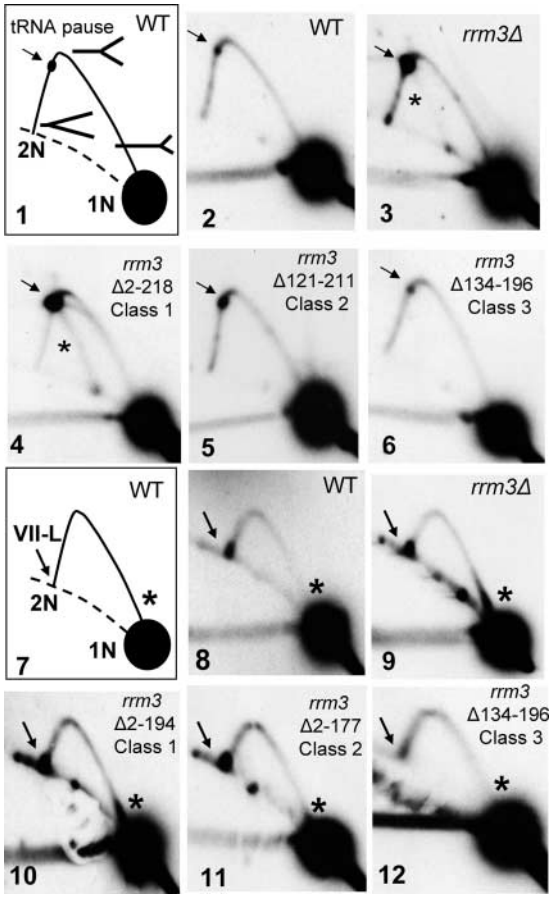

FIGURE 4.—Class 1 and class 2 *rrm3* deletion alleles have impaired replication at tRNA^A and telomere VII-L. (1) Schematic of 2D gel analysis of the 5.3-kbp *Bgl*II fragment that contains tRNA^A in *RRM3* DNA. The arrow indicates the position of tRNA^A on the arc of forked replication intermediates. (7) Schematic of 2D gel analysis of the 3.8-kbp *Cla*I fragment that contains the modified telomere VII-L in a wild-type strain: the asterisk indicates a pause in subtelomeric DNA, and the arrow indicates the pause within the ~300-bp telomere. In 1 and 7, the 1*N* spot, which consists of nonreplicating DNA, falls on the arc of linear molecules (indicated with a dashed line). Almost fully replicated DNA fragments reenter the arc of linear molecules when their mass is nearly 2*N*. Although replication was examined in each deletion allele, only one example is shown from each class. DNA from the indicated strains was digested with *Bgl*II (tRNA gels) or *Cla*I (telomere gels), separated by 2D gels, and analyzed by Southern blotting using a portion of *HIS2* (for tRNA^A) or *URA3* (telomere VII-L). (2 and 8) Wild type; (3 and 9) *rrm3*Δ; (4 and 10) class 1 mutants; (5 and 11) class 2 mutants; and (6 and 12) class 3 mutant.

any of the class 2 mutants. The class 3 mutant *rrm3*Δ134-196 exhibited a replication pattern at tRNA^A indistinguishable from that of wild-type cells (Figure 4.6).

Next we examined replication through the chromosome VII-L telomere (Figure 4.7). For these experiments, the chromosome VII-L telomere was modified by insertion of *URA3* into the *ADH4* gene, which deletes the subtelomeric repeats and a portion of *ADH4*. As shown previously (IVESSA *et al.* 2002), in wild-type cells, replication forks paused as they moved through the ~300-bp tract of telomeric DNA, and this telomeric pausing was exacerbated in *rrm3*Δ cells (Figure 4.8, WT; 9, *rrm3*Δ; position of telomere indicated by arrow). Also as shown previously, another pause mapping to a site within the *adh4* gene was detected in *rrm3*Δ but not in wild-type cells (Figure 4.9; indicated with asterisk). Cells expressing class 1 *rrm3* alleles showed both the increased pausing within the VII-L telomere and the *adh4* pause, again making replication in these mutants indistinguishable from *rrm3*Δ cells (Figure 4.10). Although the four class 2 mutants had a telomere pause similar to that in *rrm3*Δ cells, the pause within *adh4* was barely detectable (Figure 4.11). Thus, as at tRNA^A, the telomere replication phenotype for class 2 mutants was intermediate between that of wild-type cells and cells lacking Rrm3p. The class 3 mutant had a telomere replication pattern similar to that of wild-type cells (Figure 4.12).

We also examined replication through the rDNA locus. *S. cerevisiae* rDNA is organized into ~150 tandem 9.1-kbp repeat units. Each repeat contains the 5S and 35S rRNA genes, a potential origin of replication (ARS), and an RFB. Even though each repeat contains an ARS, only ~20% of these ARSs are active in a given cell cycle (BREWER and FANGMAN 1988; LINSKENS and HUBERMAN 1988; PASERO *et al.* 2002). Therefore, the pattern of replication intermediates in the rDNA 2D gels is a composite of repeats that contain an active origin and repeats that are replicated from a fork initiated in another repeat.

The RFB is a unidirectional block to replication fork progression (BREWER and FANGMAN 1988; LINSKENS and HUBERMAN 1988). When leftward moving forks encounter the RFB, they arrest. This arrest appears as an area of intense hybridization on the arc of forked replication intermediates (Figure 5, 1 and 2; marked by bracket). When a rightward moving fork converges on the leftward fork arrested at the RFB, an X-shaped structure is formed (Figure 5, 1 and 2; marked with X). In the absence of Rrm3p, the amount of DNA in converged forks increases (IVESSA *et al.* 2000). In addition, sites that do not cause replication fork slowing in wild-type cells are pause sites in *rrm3*Δ cells (IVESSA *et al.* 2000). In *rrm3*Δ cells, rightward moving forks pause at the RFB, near the beginning and end of the 35S rRNA gene, near the 5S rRNA gene, and at inactive origins (Figure 5.3; for mapping of pause sites, see IVESSA *et al.* 2000).

To examine rDNA replication, DNA was digested with *Bgl*II, which produces a 4.5-kbp fragment with the RFB in the middle of the fragment. Because of the pausing of rightward moving forks at the RFB (in addition to the arrest of leftward moving forks at this site), the amount of signal at the RFB in *Bgl*II-digested DNA is about two times higher in *rrm3*Δ cells than in wild-type cells (IVESSA *et al.* 2000; TORRES *et al.* 2004a). rDNA replication in cells expressing class 1 alleles (*rrm3*Δ2-249, *rrm3*Δ2-234, *rrm3*Δ2-218, and *rrm3*Δ2-194) had the

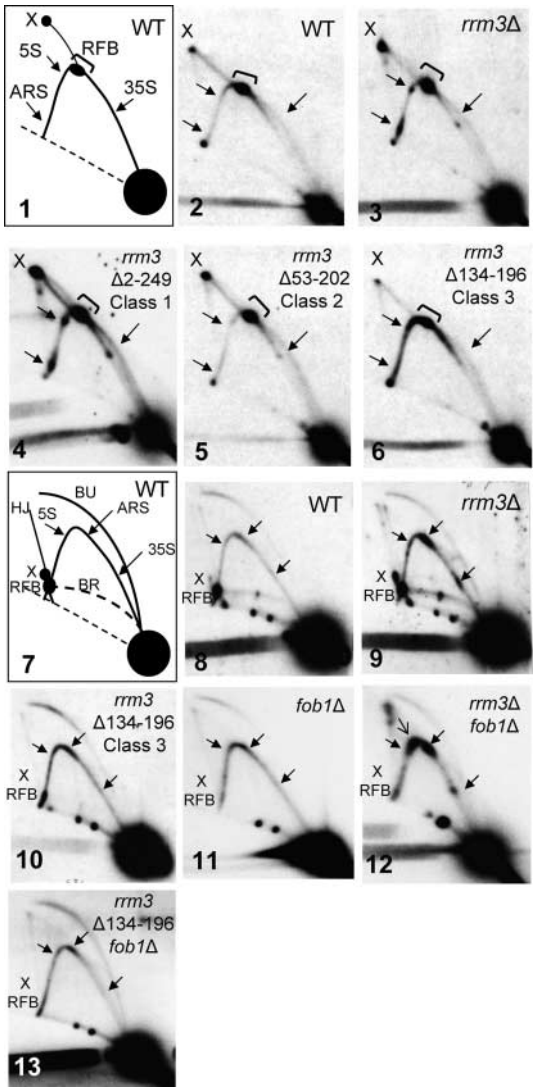

FIGURE 5.—Class 1 and class 2 *rrm3* deletion alleles have impaired replication at rDNA. (1) Schematic of 2D gel analysis of the 4.5-kbp *Bgl*II rDNA fragment in *RRM3* DNA. The positions of forks arrested (RFB; marked by bracket) and converged (X) at the RFB are indicated. Arrows mark the positions of replication forks at inactive origins of DNA replication (ARS), the end of the 35S transcript (35S), and the 5S rRNA gene (5S). (7) Schematic of 2D gel analysis of the 5.0-kbp *Stu*I rDNA fragment in *RRM3* DNA; symbols are the same as in 1. In addition, HJ indicates putative Holliday junctions, BR indicates broken replication intermediates, and BU indicates bubble-shaped replication intermediates that arise from the ~20% of repeats that contain an active origin. Although rDNA replication was examined in each deletion allele, only one example is shown from each class. DNA from the indicated strains was digested with *Bgl*II (2–6) or *Stu*I (8–13), separated by 2D gels, and analyzed by Southern blotting using a portion of rDNA as a probe. (2 and 8) Wild type; (3 and 9) *rrm3*Δ; (4) class 1 mutant; (5) class 2 mutant; and (6 and 10) class 3 mutant. To determine if the RFB phenotype of *rrm3*Δ134-196 cells was Fob1p dependent, *Stu*I-digested DNA from *fob1*Δ (11), *rrm3*Δ *fob1*Δ (12), and *rrm3*Δ134-196 *fob1*Δ (13) was analyzed. The thin arrow in 12 indicates the presence of a new pause in *rrm3*Δ *fob1*Δ cells (TORRES *et al.* 2004a).

same rDNA replication pattern as in *rrm3*Δ cells (Figure 5.4). The class 2 mutants (*rrm3*Δ2-177, *rrm3*Δ3-139, *rrm3*Δ121-211, and *rrm3*Δ53-202) again had a phenotype between that of wild-type and that of *rrm3*Δ cells (Figure 5.5). Converged forks were more abundant than in wild-type cells but less frequent than in *rrm3*Δ cells. Additionally, replication forks paused at most of the *rrm3*Δ-dependent sites, but the extent of pausing was lower than in *rrm3*Δ cells. The class 3 mutant *rrm3*Δ134-196 exhibited a unique rDNA phenotype (Figure 5.6). In this mutant, pausing at the RFB was not localized to a discrete spot but rather occurred over a larger area surrounding the RFB. In addition, there were even fewer converged forks than in wild-type cells, while all other deletion alleles showed more converged forks. In addition, pauses at the ARS, 5S, and 35S genes were not detected.

To confirm the novel RFB phenotype in the class 3 mutant, we examined rDNA replication in *rrm3*Δ134-196 cells after digestion with *Stu*I. This digest produces a fragment of ~5.0 kbp in which the ARS is in the middle of the fragment. The subset of repeats with active origins generates bubble-shaped replication intermediates (Figure 5.7; BU). Forks stalled or converged at the RFB migrate on the arc of forked intermediates near the position of fully replicated (2*N*) molecules (Figure 5.7; RFB and X). As in *Bgl*II-digested DNA, the RFB appeared less discrete in *Stu*I-digested DNA from *rrm3*Δ134-196 cells than in wild-type cells, and again, converged forks were almost absent. Pausing was not detectable at the 5S, 35S, and ARS sites, and the frequency of initiation was not detectably altered (Figure 5.10; compare to 8 and 9).

The class 3 mutant phenotype is Fob1p dependent: Fob1p binds to the RFB (HUANG and MOAZED 2003) and is essential for RFB function (KOBAYASHI and HORIUCHI 1996). In the *rrm3*Δ134-196 mutant, fork arrest at the RFB appeared less efficient: the RFB pause was less discrete than in wild-type cells, and forks did not converge at the RFB (Figure 5.6 and 10). One possible explanation for this result is that Fob1p does not bind or binds less well to the RFB in this mutant. To test this possibility, we used ChIP to monitor Fob1p binding. We used a Fob1p-Myc13-tagged protein that functions as well as wild-type Fob1p to arrest forks at the RFB (J. Z. TORRES and V. A. ZAKIAN, unpublished results). Chromatin was crosslinked *in vivo*, sheared, and immunoprecipitated with anti-Myc antibody. The crosslinks in the immunoprecipitate were reversed, and the DNA in the pellet was amplified by quantitative multiplex PCR, using primers that amplify a 363-bp fragment that spans the RFB and a 407-bp fragment from within the 35S coding region (Figure 6A). In wild-type cells, the RFB was enriched 9.6 ± 2.5-fold (average ± SD) over its presence in the no Myc tag control strain. In *rrm3*Δ134-196 cells, the RFB was enriched 13.6 ± 3.7 (Figure 6B). These values are not significantly different by the

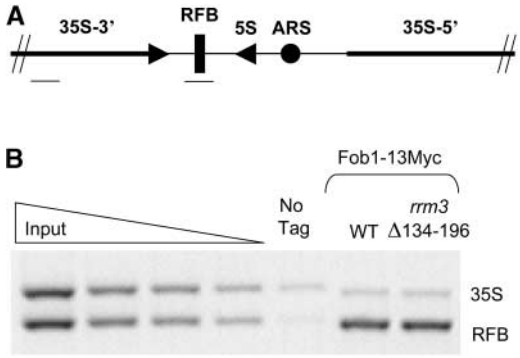

FIGURE 6.—Fob1p binding to the RFB is not diminished in *rrm3*Δ134-196 cells. (A) Schematic of a single repeat of *S. cerevisiae* rDNA. The DNA regions PCR amplified in the ChIP assays are indicated below. (B) Chromatin immunoprecipitation using anti-Myc monoclonal antibody was carried out in wild-type and *rrm3*Δ134-196 cells expressing Fob1-13Myc and in wild-type cells lacking an Myc-tagged protein (labeled no tag). Twofold serial dilutions of *rrm3*Δ input DNA were amplified to establish the linearity of PCR reaction. A 363-bp fragment that spans the complete RFB (RFB) and a 407-bp sequence from within the 35S RNA gene (35S) were PCR amplified. PCR products were resolved on a 2.8% ethidium bromide/agarose gel and quantified by densitometric analysis.

criterion of a *t*-test ($P < 0.05$). *rrm3*Δ cells also showed a similar level of Fob1p association at the RFB (J. B. BESSLER and V. A. ZAKIAN, unpublished results). Fob1p binding was specific for the RFB, as the 35S sequence was not enriched in the anti-Myc immunoprecipitate from either strain (Figure 6B). Thus, the altered pattern of replication through the RFB in *rrm3*Δ134-196 was not due to impaired Fob1p binding.

As shown previously (TORRES *et al.* 2004a), the two *rrm3*Δ-dependent defects at the RFB, the pausing of rightward moving forks, and the large increase in converged forks are Fob1p dependent (Figure 5.11). However, other *rrm3*Δ-dependent rDNA pauses, such as the pause at inactive ARSs, are not diminished in a *fob1*Δ *rrm3*Δ strain (TORRES *et al.* 2004a). In addition, there is a new pause in *fob1*Δ *rrm3*Δ rDNA that was not detected in either wild-type or *rrm3*Δ cells (Figure 5.12; leftward moving forks pausing at an inactive ARS is indicated by thin arrowhead; TORRES *et al.* 2004a). Additional new pauses are seen with different digests (TORRES *et al.* 2004a). These pauses are attributed to the passage of leftward moving forks past parts of the rDNA through which they do not normally move, as normally leftward forks are arrested at the RFB by Fob1p.

The unusual pattern of rDNA replication in the *rrm3*Δ134-196 strain might be due to pausing at a new site in rDNA. Alternatively, the novel replication pattern near the RFB in the *rrm3*Δ134-196 strain could be due to altered replication through the RFB. If the second model is correct, the elongated pause around the RFB should be Fob1p dependent. To test this possibility, we examined rDNA replication in a *fob1*Δ *rrm3*Δ134-196 strain (Figure 5.13). This mutant had a replication pattern that was indistinguishable from a *fob1*Δ strain (Figure 5.11). Thus, the presence of a functional RFB was necessary for the unusual rDNA replication pattern of the *rrm3*Δ134-196 mutant.

The amino terminus of Rrm3p is required for viability in the absence of DNA repair proteins: The pausing and breakage of replication forks that characterize *rrm3*Δ cells make them dependent upon checkpoint and repair proteins for viability (see Introduction). For example, *mec1*Δ *sml1*Δ *rrm3*Δ cells are not viable at 23° (IVESSA *et al.* 2003). [All *mec1*Δ strains used in this study are also *sml1*Δ as *mec1*Δ *sml1*Δ strains are viable but checkpoint defective (ZHAO *et al.* 1998)]. Similarly, *rrm3*Δ *srs2*Δ and *rrm3*Δ *rad50*Δ cells are not viable (IVESSA *et al.* 2003; OOI *et al.* 2003; WEITAO *et al.* 2003; SCHMIDT and KOLODNER 2004; TORRES *et al.* 2004b).

To determine if the amino terminus of Rrm3p is needed for viability when cells are checkpoint or repair deficient, we asked if cells carrying the *rrm3* amino-terminal deletion alleles as their only copy of *RRM3* were viable in the absence of Mec1p, Srs2p, or Rad50p. The deletion alleles were introduced on the *LEU2* plasmid YCplac111 into *rrm3*Δ cells that also lacked *MEC1 SML1*, *SRS2*, or *RAD50*. These strains carried a wild-type copy of *RRM3* on the *URA3* plasmid pIA20. Because cells expressing Ura3p are not viable on medium containing the drug 5-FOA (BOEKE *et al.* 1987), only cells that retain viability upon loss of pIA20 and thus have only mutant Rrm3p will grow on 5-FOA media. The *rrm3*Δ *mec1*Δ *sml1*Δ cells carrying the largest amino-terminal deletions (class 1 alleles: *rrm3*Δ2-249, *rrm3*Δ2-234, *rrm3*Δ2-218, and *rrm3*Δ2-194) did not grow on 5-FOA medium, while strains expressing class 2 and class 3 alleles were viable in the absence of Mec1p (*rrm3*Δ2-177, *rrm3*Δ3-139, *rrm3*Δ134-196, *rrm3*Δ121-211, and *rrm3*Δ53-202; for ease of presentation, only one example from each mutant class is shown in Figure 7A). The *mec1*Δ *sml1*Δ strains expressing class 2 and class 3 alleles grew as well as *RRM3 mec1*Δ *sml1*Δ cells (data not shown). The same result was obtained with *rrm3*Δ *srs2*Δ and *rrm3*Δ *rad50*Δ cells: *srs2*Δ and *rad50*Δ cells expressing class 1 *rrm3* alleles were not viable, while *srs2*Δ and *rad50*Δ strains expressing class 2 and 3 alleles were viable and grew as well as singly mutant strains (data not shown). Thus, the amino terminus of Rrm3p is required to prevent lethality in the absence of checkpoint or repair proteins. However, as little as 72 amino acids of the Rrm3p amino terminus, as in *rrm3*Δ2-177, were sufficient for viability in checkpoint- or repair-deficient *rrm3*Δ cells.

Activation of the intra-S-phase checkpoint requires the Mec1p-dependent phosphorylation of the kinase Rad53p. Rad53p hyperphosphorylation can be visualized as the presence of higher molecular weight forms of Rad53p on a Western blot (SANCHEZ *et al.* 1996). Extracts were prepared from *rrm3*Δ cells carrying a centromere plasmid without an insert or the same plasmid

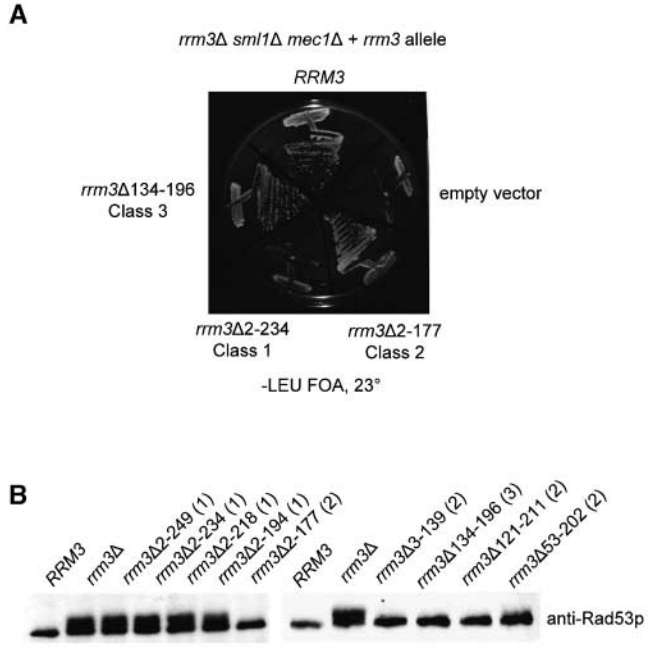

FIGURE 7.—Class 1 alleles, unlike class 2 and 3 alleles, hyperphosphorylate Rad53p and require checkpoint and repair proteins for viability. (A) A *mec1*Δ *sml1*Δ derivative of each *rrm3* deletion allele was constructed. Each strain also contained the *RRM3 URA3* plasmid pIA20. Cells were streaked on plates containing 5-FOA, which kills *URA3* cells, and grown for 3 days at 23°. Only cells that retain viability upon loss of the *URA3* plasmid-borne *RRM3* allele can grow on 5-FOA plates. One example of each deletion class is shown. (B) Cell extracts were prepared from equal numbers of log phase cultures of the indicated strains, separated on acrylamide gels, and analyzed by Western blotting using a Rad53p polyclonal antibody JDI47 kindly supplied by J. Diffley.

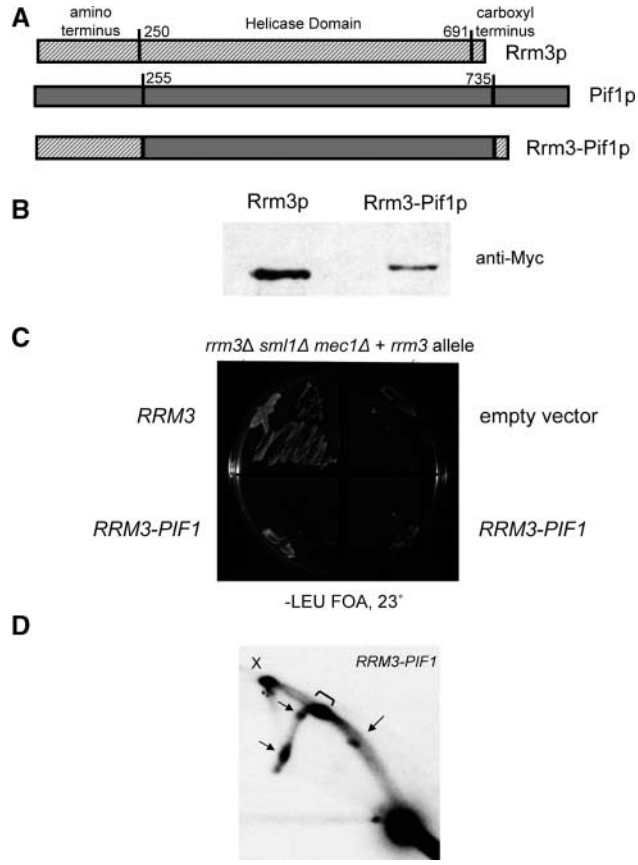

FIGURE 8.—The helicase domain contributes to the functional specificity of Rrm3p. (A) Schematic of the hybrid protein. The top line shows Rrm3p divided into its three regions. The second line shows Pif1p. In both cases, the numbers indicate the first and last amino acid of the respective helicase domain. Rrm3p is 723 amino acids long and Pif1p is 859 amino acids. The third line is the hybrid protein. Hatched regions are from Rrm3p and solid regions are from Pif1p. (B) Protein levels of wild-type protein *vs.* the Rrm3-Pif1 fusion protein. The Western blot was probed with anti-Myc monoclonal antibody. (C) Viability assay using an *rrm3*Δ *mec1*Δ *sml1*Δ strain. Strains were grown at 23° for 3 days on YC-LEU 5-FOA media. Two independent transformants of Rrm3-Pif1p are shown. (D) A 2D gel of *Bgl*II-digested DNA from *rrm3*Δ cells expressing Rrm3-Pif1p. X indicates the converged forks and the bracket marks the position of the RFB. Arrows point to the position of the 5S rRNA genes, the 35S rRNA termination site, and the ARS on the arc of simple Y's.

with either wild-type *RRM3* or one of the *rrm3* deletion alleles. These extracts were examined by Western blotting, using an anti-Rad53p serum (Figure 7B). As reported previously (IVESSA *et al.* 2003), Rad53p from *RRM3* cells migrated as a discrete band but was hyperphosphorylated in extracts from *rrm3*Δ cells. The extent of Rad53p hyperphosphorylation in cells expressing class 1 amino-terminal deletion alleles (*rrm3*Δ2-249, *rrm3*Δ2-234, *rrm3*Δ2-218, and *rrm3*Δ2-194) was indistinguishable from that of *rrm3*Δ cells. However, Rad53p was not fully phosphorylated in any of the class 2 or the class 3 deletion alleles (Rad53p might be partially activated in *rrm3*Δ53-202 cells; Figure 7B). Thus, even though cells expressing class 2 mutant alleles showed replication defects at multiple *rrm3*-dependent loci (summarized in Figure 2B), the extent of replication pausing in these mutants was not sufficient to fully activate the intra-S-phase checkpoint.

The helicase domains of Rrm3p are also required for helicase specificity: This article shows that the amino terminus of Rrm3p is needed for its replication function at $tRNA^A$, telomere VII-L, and the rDNA (Figures 4 and 5). While Rrm3p and Pif1p are 60% similar within their helicase domains, their amino termini are not related, and their *in vivo* functions are quite different (see Introduction). To determine if the amino terminus of Rrm3p confers functional specificity on its helicase domain, we generated an Myc-tagged hybrid protein consisting of the Rrm3p amino terminus, the Pif1p helicase domain, and the Rrm3p carboxyl terminus and expressed it from the *RRM3* promoter (Figure 8A). Because the helicase domain of Pif1p is 41 amino acids larger than the corresponding region of Rrm3p, this hybrid protein was 41 amino acids longer than wild-type Rrm3p. We do not know if the Pif1p helicase domain in the Rrm3-Pif1

fusion protein has helicase activity *in vitro*; the helicase domains of both Rrm3p and the *Schizosaccharomyces pombe* Pfh1p have helicase activity comparable to full-length Pif1p (Zhou *et al.* 2000, 2002; Ivessa *et al.* 2002). Western analysis revealed that this fusion protein was expressed at modestly reduced levels compared to wild-type Rrm3p (Figure 8B). A Pif1p amino terminus-Rrm3p helicase domain hybrid protein was also constructed. Although DNA sequencing confirmed that the clone was properly constructed, by the criterion of Western analysis, this fusion protein was not expressed.

Several experiments were done to determine if the Rrm3-Pif1 fusion protein could supply the replication function of Rrm3p. First, we asked if the hybrid protein could suppress the inviability of cells deleted for *RRM3* in conjunction with *srs2*Δ, *rad50*Δ or *mec1*Δ *sml1*Δ. In each case, the doubly mutant cells were inviable without the plasmid-borne *RRM3* (Figure 8C and data not shown). The inability of the Rrm3-Pif1 fusion protein to support viability held true even when the fusion protein was expressed at higher levels by placing the construct on a multicopy 2μ plasmid (data not shown). We also examined rDNA replication in cells expressing the hybrid protein. Cells expressing the hybrid protein had an rDNA replication phenotype indistinguishable from that of *rrm3*Δ cells (Figure 8D). Taken together, these data indicate that the helicase domain of Rrm3p also contributes to functional specificity.

DISCUSSION

Although Pif1 helicase family members are highly similar throughout their helicase domains, their amino termini are diverse. For example, the two *S. cerevisiae* Pif1 family members, Pif1p and Rrm3p, are 60% similar within their ~450-amino-acid helicase domain but have no significant similarity within their ~250-amino-acid amino termini (Figure 1). Since a truncated Rrm3p that lacks the first 194 amino acids of the protein has ATPase and 5′ to 3′ DNA helicase activity, the amino terminus is not required for *in vitro* activity (Ivessa *et al.* 2002). This article examines the *in vivo* function of the Rrm3p amino terminus. We constructed a series of alleles that lacked all or part of the amino terminus of Rrm3p (Figure 2A) and tested their ability to support fork progression at three Rrm3p-dependent loci, to suppress activation of DNA checkpoints, and to maintain viability in the absence of checkpoint and repair genes.

By each of these *in vivo* assays, the amino terminus of Rrm3p was essential for Rrm3p function. Strains expressing the four largest amino-terminal deletion alleles, which contained 0–55 amino acids of the amino terminus, had phenotypes indistinguishable from an *rrm3*Δ strain: cells expressing these class 1 alleles showed *rrm3*Δ-like levels of replication fork pausing at rDNA, at telomeric and subtelomeric loci, and at $tRNA^A$ (Figures 4 and 5), as well as hyperphosphorylation of Rad53p and inviability when *MEC1*, *SRS2*, or *RAD50* was deleted (Figure 7). As all of the deletion proteins were expressed, their mutant phenotypes cannot be attributed to lack of protein. Indeed, each of the class 1 alleles was expressed at levels that were roughly 10–100 times higher than wild-type Rrm3p levels (Figure 3; summarized in Figure 2B) and in some cases degradation products were visible. Similarly, amino-terminally deleted versions of Sgs1p are overexpressed and often degraded (Mullen *et al.* 2000). However, we do not believe the degradation products account for the phenotypes described in this article, as the presence of the smaller proteins did not correlate with any set of phenotypes. For example, *rrm3*Δ2-234 had almost no degradation products, while *rrm3*Δ2-194 showed extensive degradation (Figure 3). Nonetheless, cells expressing these alleles had indistinguishable phenotypes (Figure 2B).

Additionally, although we cannot rule out the possibility that the mutant phenotypes of the class 1 alleles were due to protein overexpression, we consider this interpretation unlikely, as overexpression of full-length Rrm3p from a high-copy-number 2μ plasmid did not affect DNA replication by 2D gels (J. B. Bessler and V. A. Zakian, unpublished results). Also, none of the class 1 alleles had an evident effect on growth rates while very high level overexpression of Rrm3p from a galactose-inducible promoter inhibits cell growth (J. Z. Torres and V. A. Zakian, unpublished results). In contrast to the effects of deleting parts of the amino terminus, point mutations in conserved helicase motifs that eliminate *in vivo* Rrm3p function modestly reduce Rrm3p abundance (J. B. Bessler, A. L. Garfall and V. A. Zakian, unpublished results; Ivessa *et al.* 2000). Thus, in addition to its role in promoting replication, the amino terminus of Rrm3p negatively regulates protein abundance.

Another possible explanation for the null phenotypes of class 1 alleles is that these proteins fail to enter the nucleus. Although one program (predictNLS;//maple.bioc.columbia.edu/predictNLS) did not predict a nuclear localization signal (NLS) in Rrm3p, another (PSORTII;//psort.ims.u-tokyo.ac.jpl/form2.html; Nakai and Horton 1999) detected three elements that meet the minimal criteria for an NLS (at amino acids 106, 186, and 204; Figure 1, putative NLSs are underlined). If the null phenotypes of class 1 alleles are due solely to their failure to be nuclear localized, then there must be an NLS between amino acids 177 and 194, as *rrm3*Δ2-194 is a nonfunctional class 1 allele and *rrm3*Δ2-177 is a partially functional class 2 allele and therefore must be able to enter the nucleus. Indeed, one of the minimal NLS elements predicted by PSORTII is in this region. However, *rrm3*Δ53-202 is also a class 2 allele so it too must be nuclear localized yet this allele lacks amino acids 177–194. Therefore, to explain the functionality of the different amino-terminal deletion alleles by the presence or absence of an NLS, one must invoke a second

NLS in amino acids 1–53. However, this region is not predicted to have even a minimal NLS. Thus, it is difficult to explain the phenotypes of the *rrm3* amino-terminal deletion alleles by nuclear localization alone. Moreover, at least the smallest deletion derivatives are probably small enough to enter the nucleus by diffusion. Finally, we used immunofluorescence microscopy to examine cells expressing Rrm3Δ2-249p and Rrm3Δ2-194p, the largest and smallest amino-terminal deletion derivatives that had null phenotypes, and found that neither protein was excluded from the nucleus (M. Mondoux and V. A. Zakian, unpublished results). Therefore, it is unlikely that failure to enter the nucleus is the explanation for the null phenotypes of class 1 alleles.

Class 2 alleles, which had smaller amino-terminal deletions, were also defective in DNA replication at all three loci (Figures 4 and 5). Deleting either the terminal 136 amino acids from Rrm3p (*rrm3*Δ3-139) or 90 amino acids from the center of the amino terminus (*rrm3*Δ121-211) was sufficient to reduce the ability of the protein to promote fork progression at multiple sites. However, at each locus, the extent of pausing was not as great in cells expressing class 2 alleles as it was in an *rrm3*Δ strain. Moreover, cells expressing class 2 alleles did not fully phosphorylate Rad53p nor were they dependent on Mec1p, Srs2p, or Rad50p for viability (Figure 7). Current models propose that the intra-S-phase checkpoint is activated only once the number of stalled replication forks exceeds a certain threshold (Shimada *et al.* 2002; Tercero *et al.* 2003). Our results with the class 2 *rrm3* deletion alleles support a threshold model for activation of the intra-S-phase checkpoint, as reducing the extent of replication fork pausing at the many *rrm3*-dependent pause sites obviated the dependence of class 2 mutant cells on checkpoint and repair genes and did not hyperphosphorylate Rad53p (Figure 7).

One deletion allele, *rrm3*Δ134-196, the smallest deletion examined, had a novel phenotype. In most respects, this allele was similar to wild type: replication pausing at $tRNA^A$ and telomere VII-L was comparable to that in wild-type cells, none of the *rrm3*-specific pauses in rDNA were seen, initiation of replication in rDNA was not altered, Rad53p was not hyperphosphorylated, and cells expressing this allele did not require checkpoint or repair genes for viability. However, pausing at the RFB was perturbed: the arrest at the RFB was less discrete and the abundance of forks converged at the RFB was even lower than in wild-type cells (Figure 5, 7–13). Several models can explain the phenotypes of *rrm3*Δ134-196 cells. For example, Rrm3p could play a role in forming the protein complex at the RFB, and the *rrm3*Δ134-196 protein could be defective for this function. However, this model is unlikely, as Fob1p binding to the RFB was not perturbed in *rrm3*Δ134-196 cells (Figure 6). Alternatively, the deletion could disrupt a protein interaction domain that is required for Rrm3p to recognize the RFB. This model predicts a direct interaction between RFB binding proteins and Rrm3p. Although we cannot eliminate this model, we did not detect an interaction between Fob1p and Rrm3p by co-immunoprecipitation or two-hybrid experiments (data not shown).

Another possibility is that Rrm3Δ134-196p is a more potent helicase than wild-type Rrm3p. A more active Rrm3p might increase the probability that leftward moving forks can move past the RFB-protein complex, resulting in less pausing and fewer converged forks at the RFB. This model predicts that pausing at other Rrm3p-dependent sites might also be reduced in *rrm3*Δ134-196 cells. Although we saw no suggestion for decreased pausing at $tRNA^A$ in *rrm3*Δ134-196 cells (Figure 4.6), there was a modest decrease in pausing through the VII-L telomere, although this difference was small and could not be quantitated with confidence (Figure 4; compare 12 and 8). The *rrm3*Δ134-196 allele is the only one we isolated that appears to have locus-specific effects on replication. The model that Rrm3Δ134-196p is a more active helicase is probably best tested by *in vitro* assays, but we are unable to purify Rrm3p containing large portions of its amino terminus (Ivessa *et al.* 2002). However, there is precedent for negative regulation of helicase activity by a portion of the amino terminus, as an amino-terminal deletion derivative of the yeast helicase Dna2p has higher specific activity by *in vitro* assays than does full-length protein (Bae *et al.* 2001). In addition, the amino terminus of Sgs1p is proposed to contain multiple activator and repressor domains, which can modulate helicase activity *in vivo* (Mullen *et al.* 2000). The presence of repressor and activator domains in the amino terminus of Rrm3p would also explain the intermediate phenotypes of the class 2 alleles. These domains could be protein interaction sites or affect protein folding and hence helicase activity.

We also constructed a fusion protein consisting of the Rrm3p amino terminus fused to the helicase domain of the highly related Pif1p (Figure 8). The failure of the Rrm3-Pif1 fusion protein to supply Rrm3p function is unlikely due to insufficient protein, as the very small amount of Rrm3p expressed from a galactose-inducible promoter in glucose grown cells is sufficient to confer viability on an *rrm3 sgs1* strain (J. Z. Torres and V. A. Zakian, unpublished results). Additionally, the fusion protein failed to supply Rrm3p function even when overexpressed from a high copy plasmid. These data suggest that both the amino terminus and the specific amino acid sequence of its helicase domain are required to enable Rrm3p to promote fork progression.

The data in this article show that the amino terminus is a negative regulator of Rrm3p abundance and also is required for the role of Rrm3p in moving replication forks past protein-DNA complexes. Most of the amino terminus is required for these *in vivo* functions, as deleting as little as 90 amino acids, as in *rrm3*Δ121-211, reduced its replication activity at multiple loci. The requirement for the amino terminus did not map to a

single locus: deletion of a 90-amino-acid internal segment (*rrm3*Δ121-211) or the amino-terminal 136 amino acids (*rrm3*Δ3-139) had similar phenotypes yet these deletions were largely nonoverlapping. What is the function of the amino terminus? One appealing possibility is that it serves as a binding site for one or more proteins. For example, PCNA binds to the amino terminus of Rrm3p by both two-hybrid and *in vitro* experiments, and this binding requires the terminal 54 amino acids of Rrm3p (Schmidt *et al.* 2002). A candidate PCNA interaction motif or PIP-box is present in the amino terminus of Rrm3p, spanning amino acids 35–42 (Figure 1). However, mutating the PIP-box from FF to AA in the context of full-length Rrm3p did not affect rDNA replication by 2D gel analysis (data not shown), although this mutation does reduce the two-hybrid interaction (Schmidt *et al.* 2002). Therefore, PCNA binding might not be essential for Rrm3p function or, alternatively, PCNA might bind to the amino terminus of Rrm3p at a site other than or in addition to the putative PIP box. Identifying other proteins that interact with the amino terminus of Rrm3p, as well as further *in vitro* analysis of Rrm3p, is likely to provide insight into the mechanisms used by Rrm3p to promote fork progression through protein-DNA complexes. Additionally, these analyses will further our understanding of the regulation of helicase activities.

We thank J. Diffley for the anti-Rad53 antibody, M. Rose for the anti-actin antibody, and A. Pellicioli and M. Foiani for advice on detecting Rad53p phosphorylation. We are especially grateful to M. Mondoux who examined the subcellular localization of amino truncated versions of Rrm3p. We thank A. Ivessa and B. Lenzmeier for assistance with 2D gels, J. Torres for strains and for development of the Fob1p ChIP assay, and J. Sullivan, A. Garfall, and S. Schnakenberg for assistance with some of the experiments. We also thank A. Ivessa, B. Lenzmeier, J. Torres, M. Mateyak, and B. Wardleworth for numerous helpful discussions over the course of this work and M. Mateyak, M. Sabourin, B. Wardleworth, and J.-B. Boulé for comments on the manuscript. This work was supported by grant R37 GM-26938 from the National Institutes of Health and a New Jersey Commission on Cancer Fellowship to J.B.B.

LITERATURE CITED

Bae, S. H., J. A. Kim, E. Choi, K. H. Lee, H. Y. Kang *et al.*, 2001 Tripartite structure of Saccharomyces cerevisiae Dna2 helicase/endonuclease. Nucleic Acids Res. **29:** 3069–3079.

Bennett, R. J., M. F. Noirot-Gros and J. C. Wang, 2000 Interaction between yeast sgs1 helicase and DNA topoisomerase III. J. Biol. Chem. **275:** 26898–26905.

Bessler, J. B., J. Z. Torres and V. A. Zakian, 2001 The Pif1p subfamily of helicases: region specific DNA helicases. Trends Cell Biol. **11:** 60–65.

Boeke, J. D., J. Trueheart, G. Natsoulis and G. R. Fink, 1987 5-Fluoroorotic acid as a selective agent in yeast molecular genetics. Methods Enzymol. **154:** 164–175.

Brewer, B. J., and W. L. Fangman, 1987 The localization of replication origins on ARS plasmids in S. cerevisiae. Cell **51:** 463–471.

Brewer, B. J., and W. L. Fangman, 1988 A replication fork barrier at the 3′ end of yeast ribosomal RNA genes. Cell **55:** 637–643.

Deshpande, A. M., and C. S. Newlon, 1996 DNA replication fork pause sites dependent on transcription. Science **272:** 1030–1033.

Foury, F., and J. Kolodynski, 1983 pif mutation blocks recombination between mitochondrial rho+ and rho− genomes having tandemly arrayed repeat units in Saccharomyces cerevisiae. Proc. Natl. Acad. Sci. USA **80:** 5345–5349.

Gangloff, S., J. P. McDonald, C. Bendixen, L. Arthur and R. Rothstein, 1994 The yeast type I topoisomerase Top3 interacts with Sgs1, a DNA helicase homolog: a potential eukaryotic reverse gyrase. Mol. Cell. Biol. **14:** 8391–8398.

Gietz, R. D., and A. Sugino, 1988 New yeast-Escherichia coli shuttle vectors constructed with in vitro mutagenized yeast genes lacking six-base pair restriction sites. Gene **74:** 527–534.

Gorbalenya, A. E., and E. V. Koonin, 1993 Helicases: amino acid sequence comparisons and structure-function relationships. Curr. Opin. Struct. Biol. **3:** 419–429.

Huang, J., and D. Moazed, 2003 Association of the RENT complex with nontranscribed and coding regions of rDNA and a regional requirement for the replication fork block protein Fob1 in rDNA silencing. Genes Dev. **17:** 2162–2176.

Huang, S., B. Li, M. D. Gray, J. Oshima, I. S. Mian *et al.*, 1998 The premature ageing syndrome protein, WRN, is a 3′→5′ exonuclease. Nat. Genet. **20:** 114–116.

Ivessa, A. S., J.-Q. Zhou and V. A. Zakian, 2000 The Saccharomyces Pif1p DNA helicase and the highly related Rrm3p have opposite effects on replication fork progression in ribosomal DNA. Cell **100:** 479–489.

Ivessa, A. S., J.-Q. Zhou, V. P. Schulz, E. M. Monson and V. A. Zakian, 2002 Saccharomyces Rrm3p, a 5′ to 3′ DNA helicase that promotes replication fork progression through telomeric and sub-telomeric DNA. Genes Dev. **16:** 1383–1396.

Ivessa, A. S., B. A. Lenzmeier, J. B. Bessler, L. K. Goudsouzian, S. L. Schnakenberg *et al.*, 2003 The Saccharomyces cerevisiae helicase Rrm3p facilitates replication past nonhistone protein-DNA complexes. Mol. Cell **12:** 1525–1536.

Keil, R. L., and A. D. McWilliams, 1993 A gene with specific and global effects on recombination of sequences from tandemly repeated genes in *Saccharomyces cerevisiae*. Genetics **135:** 711–718.

Kobayashi, T., and T. Horiuchi, 1996 A yeast gene product, Fob1 protein, required for both replication fork blocking and recombinational hotspot activities. Genes Cells **1:** 465–474.

Linskens, M. H. K., and J. A. Huberman, 1988 Organization of replication of ribosomal DNA in Saccharomyces cerevisiae. Mol. Cell. Biol. **8:** 4927–4935.

Longtine, M., A. I. McKenzie, D. Demarini, N. Shah, A. Wach *et al.*, 1998 Additional modules for versatile and economical PCR-based gene deletion and modification in Saccharomyces cerevisiae. Yeast **14:** 953–961.

Martin-Parras, L., P. Hernandez, M. L. Martinez-Robles and J. B. Schvartzman, 1992 Initiation of DNA replication in ColE1 plasmids containing multiple potential origins of replication. J. Biol. Chem. **267:** 22496–22505.

Mullen, J. R., V. Kaliraman and S. J. Brill, 2000 Bipartite structure of the SGS1 DNA helicase in Saccharomyces cerevisiae. Genetics **154:** 1101–1114.

Myung, K., C. Chen and R. D. Kolodner, 2001 Multiple pathways cooperate in the suppression of genome instability in Saccharomyces cerevisiae. Nature **411:** 1073–1076.

Nakai, K., and P. Horton, 1999 PSORT: a program for detecting sorting signals in proteins and predicting their subcellular localization. Trends Biochem. Sci. **24:** 34–36.

Nicholas, K. B., and H. B. J. Nicholas, 1997 Gene Doc: a tool for editing and annotating multiple sequence alignments (www.psc.edu/biomed/genedoc).

Ooi, S. L., D. D. Shoemaker and J. D. Boeke, 2003 DNA helicase gene interaction network defined using synthetic lethality analyzed by microarray. Nat Genet. **35:** 277–286.

Pasero, P., A. Bensimon and E. Schwob, 2002 Single-molecule analysis reveals clustering and epigenetic regulation of replication origins at the yeast rDNA locus. Genes Dev. **16:** 2479–2484.

Pellicioli, A., C. Lucca, G. Liberi, F. Marini, M. Lopes *et al.*, 1999 Activation of Rad53 kinase in response to DNA damage and its effect in modulating phosphorylation of the lagging strand DNA polymerase. EMBO J. **18:** 6561–6572.

Sanchez, Y., B. A. Desany, W. J. Jones, Q. Liu, B. Wang *et al.*, 1996 Regulation of RAD53 by the ATM-like kinases MEC1 and TEL1 in yeast cell cycle checkpoint pathways. Science **271:** 357–360.

Schmidt, K. H., and R. D. Kolodner, 2004 Requirement of Rrm3 helicase for repair of spontaneous DNA lesions in cells lacking Srs2 or Sgs1 helicase. Mol. Cell. Biol. **24:** 3213–3226.

Schmidt, K. H., K. L. Derry and R. D. Kolodner, 2002 Saccharomyces cerevisiae RRM3, a 5′ to 3′ DNA helicase, physically interacts with proliferating cell nuclear antigen. J. Biol. Chem. **277:** 45331–45337.

Schneider, S., and B. Schwer, 2001 Functional domains of the yeast splicing factor Prp22p. J. Biol. Chem. **276:** 21184–21191.

Scholes, D. T., M. Banerjee, B. Bowen and M. J. Curcio, 2001 Multiple regulators of Ty1 transposition in *Saccharomyces cerevisiae* have conserved roles in genome maintenance. Genetics **159:** 1449–1465.

Schulz, V. P., and V. A. Zakian, 1994 The Saccharomyces PIF1 DNA helicase inhibits telomere elongation and de novo telomere formation. Cell **76:** 145–155.

Shimada, K., P. Pasero and S. M. Gasser, 2002 ORC and the intra-S-phase checkpoint: a threshold regulates Rad53p activation in S phase. Genes Dev. **16:** 3236–3252.

Sikorski, R. S., and P. Hieter, 1989 A system of shuttle vectors and yeast host strains designed for efficient manipulation of DNA in *Saccharomyces cerevisiae*. Genetics **122:** 19–27.

Suzuki, N., M. Shiratori, M. Goto and Y. Furuichi, 1999 Werner syndrome helicase contains a 5′→3′ exonuclease activity that digests DNA and RNA strands in DNA/DNA and RNA/DNA duplexes dependent on unwinding. Nucleic Acids Res. **27:** 2361–2368.

Taggart, A. K. P., S.-C. Teng and V. A. Zakian, 2002 Est1p as a cell cycle-regulated activator of telomere-bound telomerase. Science **297:** 1023–1026.

Tanaka, H., G. H. Ryu, Y. S. Seo, K. Tanaka, H. Okayama *et al.*, 2002 The fission yeast pfh1$^+$ gene encodes an essential 5′ to 3′ DNA helicase required for the completion of S-phase. Nucleic Acids Res. **30:** 4728–4739.

Tercero, J. A., M. P. Longhese and J. F. Diffley, 2003 A central role for DNA replication forks in checkpoint activation and response. Mol. Cell. **11:** 1323–1336.

Torres, J. Z., J. B. Bessler and V. A. Zakian, 2004a Local chromatin structure at the ribosomal DNA causes replication fork pausing and genome instability in the absence of the S. cerevisiae DNA helicase Rrm3p. Genes Dev. **18:** 498–503.

Torres, J. Z., S. L. Schnakenberg and V. A. Zakian, 2004b The Saccharomyces cerevisiae Rrm3p DNA helicase promotes genome integrity by preventing replication fork stalling: viability of rrm3 cells requires the intra S phase checkpoint and fork restart activities. Mol. Cell. Biol. **24:** 3198–3212.

Wang, Y., and C. Guthrie, 1998 PRP16, a DEAH-box RNA helicase, is recruited to the spliceosome primarily via its nonconserved N-terminal domain. RNA **4:** 1216–1229.

Warbrick, E., 2000 The puzzle of PCNA's many partners. BioEssays **22:** 997–1006.

Weitao, T., M. Budd, L. L. Hoopes and J. L. Campbell, 2003 DNA2 helicase/nuclease causes replicative fork stalling and double-strand breaks in the ribosomal DNA of Saccharomyces cerevisiae. J. Biol. Chem. **278:** 22513–22522.

Wellinger, R. J., K. Ethier, P. Labrecque and V. A. Zakian, 1996 Evidence for a new step in telomere maintenance. Cell **85:** 423–433.

Zhao, X., E. G. Muller and R. Rothstein, 1998 A suppressor of two essential checkpoint genes identifies a novel protein that negatively affects dNTP pools. Mol. Cell **2:** 329–340.

Zhou, J.-Q., E. M. Monson, S.-C. Teng, V. P. Schulz and V. A. Zakian, 2000 The Pif1p helicase, a catalytic inhibitor of telomerase lengthening of yeast telomeres. Science **289:** 771–774.

Zhou, J.-Q., H. Qi, V. Schulz, M. Mateyak, E. Monson *et al.*, 2002 Schizosaccharomyces pombe pfh1+ encodes an essential 5′ to 3′ DNA helicase that is a member of the PIF1 sub-family of DNA helicases. Mol. Biol. Cell **13:** 2180–2191.

Ziegelin, G., T. Niedenzu, R. Lurz, W. Saenger and E. Lanka, 2003 Hexameric RSF1010 helicase RepA: the structural and functional importance of single amino acid residues. Nucleic Acids Res. **31:** 5917–5929.

Communicating editor: L. Pillus